Jefferson Lab PAC14
Proposal Cover Sheet

This document must be received by close of business Thursday, **June 4, 1998** at:

Jefferson Lab
User Liaison Office,
Mail Stop 12B
12000 Jefferson Avenue
Newport News, VA
23606

Experimental Hall: A
Days Requested for Approval: 27

☒ **New Proposal Title:** K^+ photoproduction and Λ^0 Polarization
☐ **Update Experiment Number:** ~~for~~ $E_\gamma = 3$ to 6 GeV
☐ **Letter-of-Intent Title:**
(Choose one)

Proposal Physics Goals
Indicate any experiments that have physics goals similar to those in your proposal.

Approved, Conditionally Approved, and/or Deferred Experiment(s) or proposals:

94-012
97-108
89-004
94-108
} each has some overlap, none are "similar overall".

Contact Person

Name: Meihua Liang
Institution: Jefferson Lab
Address:
Address:
City, State, ZIP/Country:
Phone: (757) 269-7176 **Fax:** x5235
E-Mail: mLiang@jlab.org

Jefferson Lab Use Only

Receipt Date: 6/4/98
By: [illegible]

PR 98-~~006~~ 106

BEAM REQUIREMENTS LIST

JLab Proposal No.: 98-106 Date: 6/4/98

Hall: A Anticipated Run Date: _____ PAC Approved Days: _____

Spokesperson: M. Liang, R. Gilman, A. Afanasa Hall Liaison: _____
Phone: (757) 269-7176
E-mail: mliang@jlab.org

List all combinations of anticipated targets and beam conditions required to execute the experiment. (This list will form the primary basis for the Radiation Safety Assesment Document (RSAD) calculations that must be performed for each experiment.)

Condition No.	Beam Energy (MeV)	Mean Beam Current (μA)	Polarization and Other Special Requirements (e.g., time structure)	Target Material (use multiple rows for complex targets — e.g., w/windows)	Material Thickness (mg/cm²)	Est. Beam-On Time for Cond. No. (hours)
1	3000	25	80%	LH_2 target (*)	1200	60
2	4000	"	"	"	"	55
3	5000	"	"	"	"	105
4	6000	"	"	"	"	64
5	3000	"	"	LH_2 + 6% Cu radiator (**)	2000	60
6	4000	"	"	"	"	55
7	5000	"	"	"	"	105
8	6000	"	"	"	"	64
			(*) Standard Hall A 15 cm LH_2 cryotarget		1.1 g/cm² H	+ 0.1 g/cm² Al
			(**) 6% Cu radiator	~ 0.78 g/cm²		

The beam energies, E_{Beam}, available are: $E_{Beam} = N \times E_{Linac}$ where N = 1, 2, 3, 4, or 5. E_{Linac} = 800 MeV, i.e., available E_{Beam} are 800, 1600, 2400, 3200, and 4000 MeV. Other energies should be arranged with the Hall Leader before listing.

HAZARD IDENTIFICATION CHECKLIST

JLab Proposal No.: 98-106 (For CEBAF User Liaison Office use only:) Date: 6/4/98

Check all items for which there is an anticipated need. Standard Hall A cryotarget setup.

Cryogenics
- _____ beamline magnets
- _____ analysis magnets
- _____ target
  - type: _____
  - flow rate: _____
  - capacity: _____

Electrical Equipment
- _____ cryo/electrical devices
- _____ capacitor banks
- _____ high voltage
- _____ exposed equipment

Radioactive/Hazardous Materials
List any radioactive or hazadorous/ toxic materials planned for use:
_____
_____
_____
_____

Pressure Vessels
- _____ inside diameter
- _____ operating pressure
- _____ window material
- _____ window thickness

Flammable Gas or Liquids
- type: _____
- flow rate: _____
- capacity: _____

Drift Chambers
- type: _____
- flow rate: _____
- capacity: _____

Other Target Materials
- ___ Beryllium (Be)
- ___ Lithium (Li)
- ___ Mercury (Hg)
- ___ Lead (Pb)
- ___ Tungsten (W)
- ___ Uranium (U)
- ✓ Other (list below)

6% Cu radiator

Vacuum Vessels
- _____ inside diameter
- _____ operating pressure
- _____ window material
- _____ window thickness

Radioactive Sources
- _____ permanent installation
- _____ temporary use
- type: _____
- strength: _____

Large Mech. Structure/System
- _____ lifting devices
- _____ motion controllers
- _____ scaffolding or
- _____ elevated platforms

Lasers
- type: _____
- wattage: _____
- class: _____

Installation:
- _____ permanent
- _____ temporary

Use:
- _____ calibration
- _____ alignment

Hazardous Materials
- ___ cyanide plating materials
- ___ scintillation oil (from)
- ___ PCBs
- ___ methane
- ___ TMAE
- ___ TEA
- ___ photographic developers
- ___ other (list below)

_____
_____

General:

Experiment Class:
- ✓ Base Equipment
- _____ Temp. Mod. to Base Equip.
- _____ Permanent Mod. to Base Equipment
- _____ Major New Apparatus

Other: _____
_____

LAB RESOURCES LIST

JLab Proposal No.: 98-106 Date 6/4/98

(For JLab ULO use only.)

List below significant resources — both equipment and human — that you are requesting from Jefferson Lab in support of mounting and executing the proposed experiment. Do not include items that will be routinely supplied to all running experiments such as the base equipment for the hall and technical support for routine operation, installation, and maintenance.

Major Installations *(either your equip. or new equip. requested from JLab)*

None

New Support Structures: None

Data Acquisition/Reduction

Computing Resources: None

New Software: None

Major Equipment

Magnets: None

Power Supplies: None

Targets: None

Detectors: None

Electronics: None

Computer Hardware: None

Other: None

Other: None

A New Proposal for Jefferson Lab Hall A, PAC 14

K^+ Photoproduction and Λ^0 Polarization for $E_\gamma = 3$ to 6 GeV

D. Geesaman
Argonne National Laboratory
M. K. Jones, C. F. Perdrisat
College of William & Mary
W. Boeglin, L. Kramer, P. Markowitz, B. Raue
Florida International University
O. K. Baker
Hampton University
J. P. Chen, E. Chudakov, K. de Jager, J. Gomez, O. Hansen, M. Kuss, J. LeRose, M. Liang (contact person), D. Mack, R. Michaels, A. Saha, B. Wojtsekhowski
Jefferson Laboratory
C.-C. Chang
University of Maryland
J. R. Calarco
University of New Hampshire
V. Punjabi
Norfolk State University
A. Afanasev (cospokesperson), B. Vlahovic
North Carolina Central University
C. E. Hyde-Wright, L. Todor
Old Dominion University
G. J. Lolos
University of Regina
R. Gilman (cospokesperson), C. Glashausser, X. Jiang, G. Kumbartzki, S. Malov, R. Ransome, S. Strauch
Rutgers University
S. Choi, S. Incerti, Z.-E. Meziani
Temple University

Abstract

We propose a coincidence measurement of K^+ and p from the $\vec{\gamma}p \rightarrow K^+\vec{\Lambda}^0$, $\Lambda^0 \rightarrow p\pi^-$ reaction, for photon energies from 3 to 6 GeV, and for K^+ angles in the center of mass from 50° to 130°. The polarized photons will be generated with a 25 μA beam of 80% longitudinally polarized electrons. The measurement of the recoil $\vec{\Lambda}^0$ polarization components P_l, P_t, and P_n will be the first polarization measurements in this energy regime, and will have statistical uncertainties $\leq \pm 0.1$. Six existing cross section points for $\theta^K_{cm} \geq 70°$ are known with uncertainties of about 50%; we overlap these points and extend the angle range, measuring 18 points with uncertainties of 5 - 10%.

Our aim is to understand the exclusive reaction mechanism, in particular to test the various quark-based reaction models that are now available. Recent theoretical advances indicate that, with these new experimental data, we should be able to:

- examine the role of spin in this reaction, since the spin of the Λ^0 is believed to be carried by the s quark, and the Λ^0 polarization is predicted to be large,
- extract information about competing reaction mechanisms, since mechanisms such as kaon knockout, kaon production from the quark, and "diffractive" kaon production are generally expected to have different spin structures,
- observe deviations from the Brodsky-Farrar constituent counting rules, since estimates of deviations are now available, and the estimated deviations can be seen with the uncertainties of this measurement, and
- learn about non-forward parton distributions, since within this framework of "soft" physics, the power-law behavior of the cross section data can be estimated.

1 Motivation

1.1 Introduction

Our experimental knowledge of exclusive photoreactions for energies above 3 GeV is extremely limited. Data [1, 2, 3] mostly date from the 1970s. The

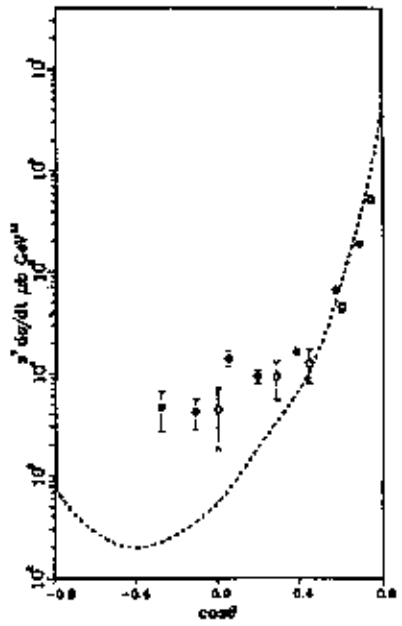

Figure 1: *Cross section data for $\gamma p \to K^+\Lambda^0$ at 4 GeV (filled circles) and 6 GeV (open circles). The cross sections have been multiplied by s^7 to show that the constituent counting rules are followed approximately. The perturbative QCD prediction is described in the theory section of the text.*

few measured cross sections for $K^+\Lambda^0$ at large angles are shown in Fig. 1. These data were measured at K^+ center of mass angles up to 110° at 4 GeV and 90° at 6 GeV, corresponding to four momentum transfer Mandelstam variable t, of -4.0 and -4.9 $(\mathrm{GeV/c})^2$, respectively. As is the case with other photoreactions, these cross sections [3] approximately follow the constituent counting rules of Brodsky and Farrar [4] :

$$\frac{d\sigma}{dt} \approx s^{2-n} f(\cos\theta_{c.m.}).$$

Here s and t are the standard Mandelstam variables. The constituent counting rules can be derived for exclusive processes at large momentum transfer from perturbative QCD. However, it is generally believed that pQCD should not apply to these reactions at a few GeV beam energy [5]. Until recently, however, no other model existed that could explain why the data apparently follow these rules.

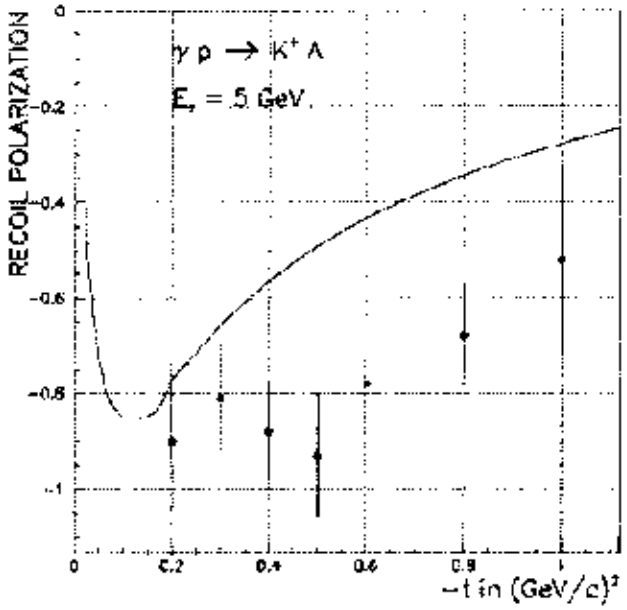

Figure 2: *Induced Λ^0 polarization data at 5 GeV photon energy, compared to a Regge theory calculation.*

There are only a few induced polarization measurements [2], most of poor quality, and all at small scattering angles, for which the four momentum transfer $-t$ is typically < 1 (GeV/c)^2. These data are shown in Fig. 2. The largest $-t$ data point corresponds to a center of mass angle of about 40°. The calculation shown, by Guidal, Laget, and Vanderhaeghen [6], uses a Regge trajectory model, with an extrapolation that satisfies scaling laws at high momentum transfers. This model is in generally good agreement with the cross section data at several energies, for $-t \leq 1$ (GeV/c)^2.

1.2 Reaction Mechanism

Our physics motivation is to test the predictions of quark-based models for $K^+\vec{\Lambda}^0$ photoproduction. The motivation has two parts, an exploration of spin physics to investigate competing reaction mechanisms, and an investigation of deviations from the constituent counting rules. Of course, the two topics are interrelated, since one needs both cross section and polarization observables to understand the physics underlying the data.

It is generally believed that $K^+\Lambda^0$ photoproduction is an ideal test case for quark-based models of spin physics. This results from the observation that the spin of the Λ^0 is carried entirely by the s quark in the constituent quark model. While this is not exactly true in the parton model, it should be approximately true as sea quark contributions are reduced in exclusive reactions.

Understanding the underlying reaction mechanism will require a number of polarization measurements. Possible reaction mechanisms in this region are illustrated in Fig. 3, and described below:

(a) *"diffractive" process*: In a vector-meson dominance picture, one expects that the incident photon can quantum-mechanically oscillate into a ϕ meson. This ϕ meson can scatter from the proton through a quark exchange mechanism, leading to a $K^-\Lambda^0$ final state. The cross section will be largest when the exchange involves the energy transfer needed to put the K^+, and the Λ^0 on shell, but very little momentum transfer, i.e. small t. Thus the K^+ preferably goes in about the same direction as the incident photon. One can think of this as a "diffractive" process, though normally this term is used to indicate the incoming vector meson scatters through Pomeron exchange.

(b) *K^+ production from a quark*: When the transverse momentum transfer

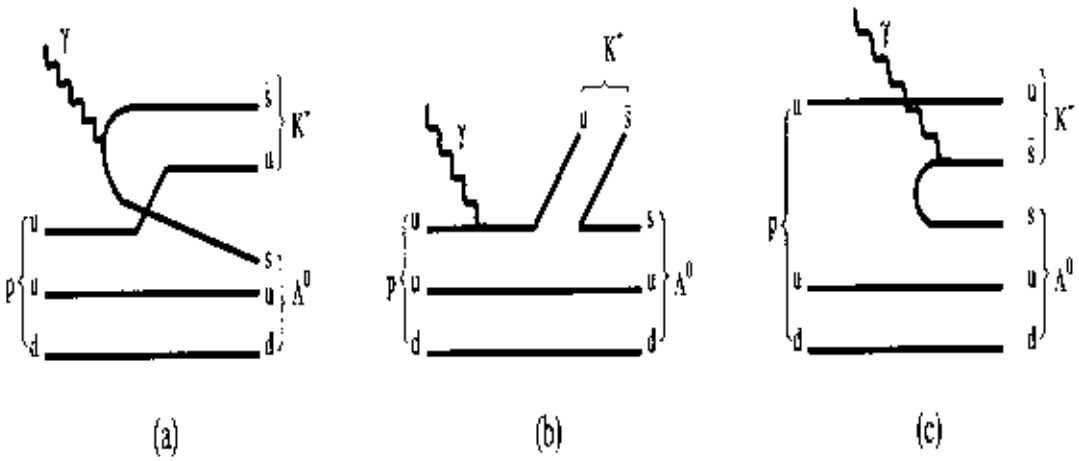

Figure 3: *Examples of Feynman diagrams for three reaction mechanisms: (a) "diffractive" process, (b) K^+ production from a quark, and (c) virtual kaons in the nucleon. See text for details.*

p_T, or the four momentum transfers $-t$ and $-u$ are large, one expects that reactions are dominated by interaction of the photon with a single quark. In kaon photoproduction, a single quark absorbs the photon, followed by meson production from the off-shell quark, for example $u \to K^+ s$. This process can be estimated within quark-based models, such as pQCD, diquark models, or in the framework of newly developed non-forward parton distribution calculations.

(c) *virtual kaons in the nucleon*: Part of the proton wave function involves components with strange sea quarks. The $s\bar{s}$ sea quarks do not have to be in a color singlet state, and one can picture that the $uuds\bar{s}$ wave function of the proton partly resembles a $K^+\Lambda^0$ state. Thus, the photon may add energy to put a preexisting $K^+\Lambda^0$ virtual state on mass shell. Though the topic of $s\bar{s}$ sea quarks in the proton is of great interest, we do not concentrate on it in this proposal as we would expect that its contribution is small, perhaps $< 10\%$, because the diagram involves

disconnected quark lines and sea quarks.

These different mechanisms are generally expected to have different spin structures, and their interference could lead to dramatic effects in the polarization observables.

1.3 Theoretical Models

Recent calculations of polarization observables and cross sections in $\vec{\gamma}p \to K^+\vec{\Lambda}^0$ have been made within several quark models. We review some of the theoretical ideas and models below.

1.3.1 Helicity conservation

In quark-based models, one usually assumes quark helicity conservation, and neglects orbital angular momentum, which leads to hadron helicity conservation. Assuming hadronic helicity conservation, the reaction can be described in terms of two non-zero complex helicity amplitudes.

There are three recoil $\vec{\Lambda}^0$ polarization components. (See [7] for notation.) The component normal to the reaction plane, P_n, results from the induced polarization: $P_n = P$. The component in the direction of the $\vec{\Lambda}^0$ momentum, P_l, is a spin transfer component that depends on the photon helicity: $P_l = hC_z$, where h is the photon helicity and C_z is the longitudinal spin transfer. The in-plane component perpendicular to the direction of the $\vec{\Lambda}^0$ momentum, P_t, is also a spin transfer component that depends on the photon helicity: $P_t = hC_x$, where C_x is the transverse spin transfer.

If helicity is conserved, we expect:

$$P = C_x = 0.$$

C_x and P result from a similar interference of helicity flip and non-flip amplitudes with one reservation: C_x selects the *real* part of the corresponding bilinear combination of the amplitudes, whereas P selects the *imaginary* part. Therefore *both* C_x and P should be measured to draw conclusions about the relative strength of helicity flip and non-flip transitions in kaon photoproduction.

Carlson and Chachkhunashvili [8] observe that constituent counting rules generally work in photoreactions for photon energies above 4 GeV, and four momentum transfers $-t$ above 3 $(\mathrm{GeV/c})^2$, but the related prediction of

helicity conservation has never been tested in this kinematic regime, where it should be applicable, if the pQCD explanation is correct. In this proposal, several of our kinematic points have photon energies and t that satisfy the criteria of [8], and could provide the first such test.

If hadronic helicity is conserved, the polarization transfer C_z can be defined in terms of the two independent helicity amplitudes as:

$$C_z = \frac{|S_2|^2 - |S_1|^2}{|S_2|^2 + |S_1|^2}$$

and is equal to the beam - target asymmetry E. The S_2 matrix element has total angular momentum $1/2$, and is given by

$$< \lambda_\gamma = 1, \lambda_p = 1/2 | O | \lambda_K = 0, \lambda_\Lambda = 1/2 >$$

where O is the appropriate operator, and λ_γ, for example, is the helicity of the γ. The S_1 matrix element has total angular momentum $3/2$, and is given by

$$< \lambda_\gamma = 1, \lambda_p = -1/2 | O | \lambda_K = 0, \lambda_\Lambda = -1/2 > .$$

From pQCD scaling arguments, C_z is constant at fixed $\theta_{c.m.}$, but helicity conservation alone does not in general determine its value within the physically allowed range between -1 and +1. Therefore, one needs a dynamical model for the reaction to predict the magnitude of C_z.

1.3.2 Kaon production from a quark

Afanasev, Carlson, and Wahlquist [9] have estimated polarization observables in a quark-based model. The meson production amplitude off a single quark is factorized out, and using pQCD for $\gamma q \to Kq$, and neglecting mass corrections, one gets the following predictions for the polarization observables:

$$E = C_z = \frac{s^2 - u^2}{s^2 + u^2}$$

$$P = C_x = 0$$

and

$$\Sigma = \frac{2su}{s^2 + u^2}$$

Here s and u are the Mandelstam variables, and Σ is the asymmetry between linearly polarized photons polarized in and perpendicular to the reaction

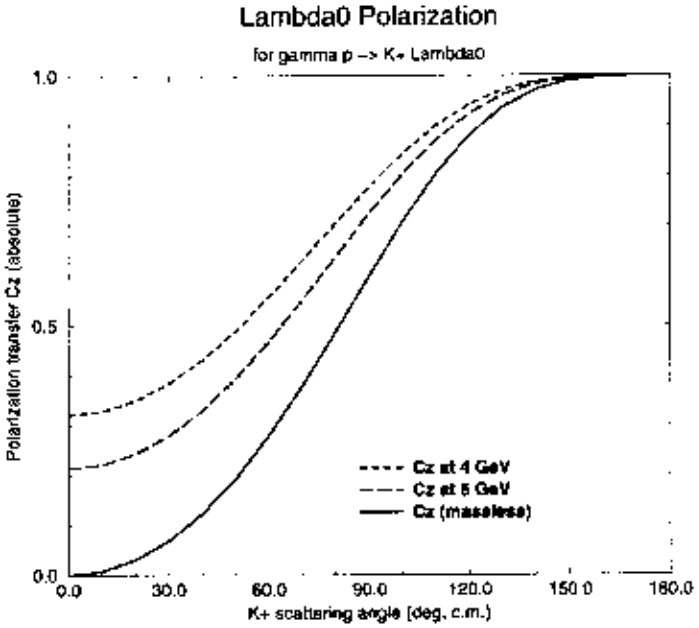

Figure 4: *Calculation of C_z, from a model of kaon production from a single quark.*

plane. This prediction is shown in Fig. 4, in the high energy limit of massless particles, and with exact values of s and u calculated for 4 and 6 GeV beam energies. At backward angles, only S_2 survives, leading to $C_z = 1$. Since the spin of the Λ is carried by the s quark, the Λ "remembers" polarization transferred from the photon to the s quark.

1.3.3 pQCD calculations

A more detailed prediction of the spin-dependent and total differential cross sections within a perturbative QCD framework was provided by Farrar, Huleihel, and Zhang [10] by explicit calculation of all lowest-order (α_s^3) Feynman diagrams. The predicted differential cross section is compared to the data of [3] in Fig. 1. Sensitivity to the distribution amplitudes was not investigated in the case of kaon photoproduction, but for pion production the overall magnitude of the cross section could vary by an order of magnitude between different distribution amplitudes. Note that such a calculation is technically involved since a few *thousand* topologically different diagrams

contribute to the amplitude in the lowest order of perturbation theory. The spin observables P_n and C_x are assumed to vanish in this calculation. The behavior of C_z appears similar to that of Fig. 4, except that the range is larger, from about -1 at forward angles to 0 at 90°, and to nearly 1 at back angles. It is difficult to make definitive comparisons, as these calculations were only done at a few angles.

1.3.4 Diquark model

Calculations of cross sections and polarization observables for $\vec{\gamma}p \to K^+\vec{\Lambda}^0$ have also been done within the diquark model by Kroll, Schurmann, Passek, and Schweiger [11]. This is a semi-phenomenological model, in which the interaction is with a single quark, with the remaining two quarks as "spectators". It has been applied successfully to, for example, moderate Q^2 nucleon form factor data. Cross section calculations are compared to data in Fig. 5. Two calculations for 4 GeV (dashed-double-dotted line) and 6 GeV (solid line) are in rough agreement with the data. These calculations use quark-diquark proton and Λ distribution amplitudes taken from previous works, and an asymptotic form for the kaon distribution amplitude. Spin-flavor SU(6) symmetry was used to derive the diquark model parameters for the Λ. One sees from the comparison of the two that deviations from scaling of about 30% are expected. The short dashed curve at the top is a calculation for 6 GeV using a CZ kaon distribution amplitude. The long-dashed curve on the bottom indicates the pQCD result by [10].

1.3.5 Non-forward parton distributions

Recently there has also been much work in the framework of non-forward parton distributions (NFPD), originally derived by Ji and Radyushkin [12]. The NFPD are used to describe the probability of emission of an interacting quark from an initial proton, and its re-absorption after the interaction. These distributions may be thought of as generalizations of the unpolarized and polarized quark / parton distribution functions from deep inelastic scattering.

Radyushkin [13] has estimated scaling power laws for real Compton scattering in the framework of NFPD. Note that in this model the calculation is purely of "soft" contributions; there are no hard gluon exchanges. He finds that the scaling power increases with angle, and that it is s^{-6}, the same as

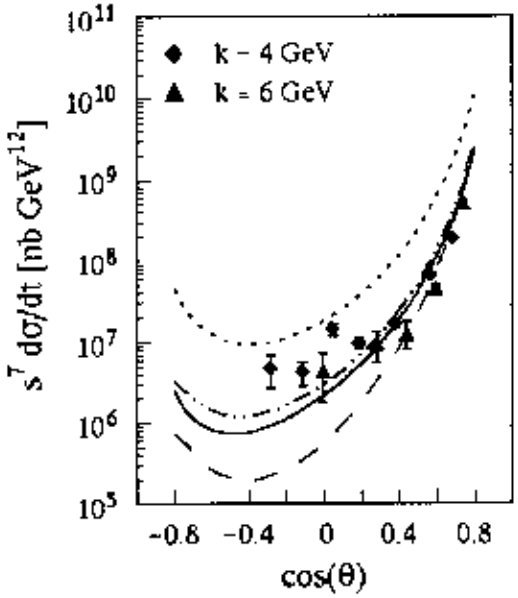

Figure 5: *Diquark model calculations of differential cross sections for* $\gamma p \to K^+\Lambda^0$.

the PQCD power law, near 130°. It is about one power of s slower at forward angles. While experimentally this may be viewed as deviations from the pQCD scaling, theoretically it is unrelated "soft" physics. Existing data have uncertainties on the power of s of typically a few tenths to one, and the existing data for real Compton scattering are too uncertain to strongly favor either pQCD scaling or the behavior predicted by Radyushkin. Radyushkin has speculated that this pattern of "scaling violation", a faster fall-off in the cross section at larger angles, will hold for other photoreactions.

Similar calculations in the framework of NFPD have also been done for meson electroproduction [14]. It has been pointed out that these reactions can be used to measure the NFPD. It is interesting to note that in pseudoscalar meson photoproduction, the *spin-dependent* NFPD of a nucleon determine the reaction amplitude, whereas the *spin-independent* NFPD determine the amplitudes of vector-meson production and Compton scattering on a nucleon. As a result, measuring pseudoscalar photoproduction gives us yet another way to examine the nucleon spin problem.

Calculations [15] are now underway to estimate kaon photoproduction cross sections and polarization observables within this framework. While

results are not available at this time, we note that within this model one still has $P_n = 0$, but one does *not* expect in general that $C_x = 0$.

1.4 Motivation Summary

Our general aim in this proposal is to test several quark models through the study of $\vec{\gamma}p \to K^+\vec{\Lambda}^0$ at large s and t. For the first time, we now have estimates, within the diquark model and the framework of non-forward parton distributions, of what deviations to expect from the constituent counting rules. Obtaining data that show such deviations would resolve a long standing puzzle: why data appear to follow pQCD scaling, in a regime where pQCD is not generally expected to be applicable.

A general conclusion from these calculations is that one may expect a large polarization transfer in kaon photoproduction, with the exact magnitude being sensitive to the model and hadronic distribution amplitudes. There are now polarization calculations within a model of kaon production off a quark, a pQCD calculation, and within the diquark model. All these models conserve helicity, an assumption that will be directly tested by our measurements of P_n and C_x, which together measure both the imaginary and real parts of the helicity-violating interference. Similar behaviors are predicted within these models for the longitudinal polarization transfer C_z; it may be that none are correct. Calculations in the framework of NFPD should be available soon.

By measuring this set of observables, there will be strong constraints on the calculation and on the underlying reaction dynamics. For real Compton scattering, for example, Vanderhaeghen [16] has pointed out that the calculation can be inverted, and one can use the data to extract distribution amplitudes. He finds that the cross section and polarization observables allow a much more precise extraction than does the cross section alone.

1.5 Related Experiments

There is no Jefferson Lab experiment of which we are aware which strongly overlaps the current proposal, but some approved experiments have potential implications for the physics studies proposed here.

Experiment 94-012 (Gilman, Holt *et al.*) will measure cross sections and polarizations for $\vec{\gamma}p \to \vec{p}\pi^0$ up to 5 GeV. Ideas concerning the role of spin and scaling violations can be addressed by this measurement, but spin predictions are not as certain in pion production, the energy range is not as large, and

calibration of the polarimeter makes it difficult to extend the $\vec{p}\pi^0$ production to higher energies.

Experiment 97-108 (Wojtsekhowski, Nathan, Hyde-Wright *et al.*) will measure cross sections for real Compton scattering, $\gamma p \to p\gamma$, for 3 to 6 GeV beam energy. Scaling violations can be addressed by this measurement, but the experiment lacks polarization measurements, which will be very difficult due to the much lower count rate.

Hall B experiment 89-004 (R. Schumacher *et al.*) studies photoproduction of $K^+\Lambda^0$, $K^+\Sigma^0$, and $K^0\Sigma^+$, at photon energies up to 3 GeV. Our proposed 3 GeV data will provide some overlap with this experiment, and the comparison will allow a check between the experiments. While the first reaction is the same as we propose to measure, the physics interests and kinematics are different from the current proposal. It would be difficult to extend the Hall B measurement to our kinematics, due to lower luminosity, difficulty in particle identification, and poorer resolution in kinematic reconstructions.

Kaon electroproduction experiments do not in general have much implication for the physics proposed here, with the possible exception of conditionally approved experiment 94-108 (Markowitz, Frullani, Iodice, Baker, Chang *et al.*). One aspect of that proposal is a measurement of unseparated cross sections as a function of t, up to t = -3 (GeV/c)^2 for Q^2 = 3.0 (GeV/c)^2 and W = 2.2 GeV. The aim is to search for the transition to pQCD / quark behavior. In contrast, our kinematics are for t from about -0.8 to -6.5 (GeV/c)^2, at $Q^2 = 0$ (GeV/c)^2 and $\sqrt{s} \sim W$ of 2.5 to 3.5 GeV. Because of the kinematic differences, the differences between photo- and electro-production, and the polarization measurements of this proposal, we and the proposers of 94-108 view these two proposals as more complementary than competitive.

2 Experimental Details

2.1 Kinematics and Uncertainties

Our goal is to test several quark models through the study of $\vec{\gamma}p \to K^+\vec{\Lambda}^0$ at large s and t. These models show slow, smooth variations of cross sections and polarizations as a function of angle. Thus we propose measurements for beam energies from 3 to 6 GeV and angles from 50° to 130° center of mass, to provide the maximum possible kinematic range with a moderate number of settings, and to be above the region of discrete resonances.

We propose to measure kaon cross sections to 5 - 10 % uncertainties (statistical plus systematic) across the kinematic range, to be able to detect deviations from the constituent counting rules of the size estimated by [11, 13]. From the diquark model, we expect 30 - 40% variations from an s^{-7} scaling behavior, with bigger deviations at larger angles. Extrapolating from Radyushkin's results in Compton scattering, the deviations should vary systematically with angle, with the biggest deviations at forward angles. One power of s slower cross-section fall-off corresponds to a factor of two increase in cross section over the constituent counting rule estimate, for our range of beam energies. Uncertainties of 5 - 10% allow determination of the power of s in the exponent to uncertainties of 0.1 - 0.2, and represent a major advance over the current data which are known to 50 % at large $-t$.

We propose to measure the recoil Λ^0 polarization components to a statistical uncertainty $\leq \pm 0.1$, typically ± 0.06. No polarization data exist in these kinematics, and our projected uncertainties are better than existing measurements at lower beam energies and smaller momentum transfers.

2.2 Coincidence Measurement

We measure $\vec{\gamma}p \to K^+\vec{\Lambda}^0$ by detecting in coincidence the K^+ and the proton from the $\Lambda^0 \to p\pi^-$ decay, as illustrated in Fig. 6. For the cross section measurement, the coincident proton, with kinematic reconstructions, allows us to identify $K^+\Lambda^0$ production. This avoids the difficult problem of particle identification of K^+ from a larger π^+ background present in singles measurements.

The proton is also used to measure the Λ^0 polarization. The $\Lambda^0 \to p\pi^-$ decay has a $64.1 \pm 0.5\%$ branching ratio, and is self-analyzing with an angular distribution in the Λ rest frame of $1 + AP_\Lambda \cos\theta$. Here θ is the angle between the proton and the Λ spin direction, A is the analyzing power, equal to 0.642 $\pm$ 0.013, and P_Λ is the Λ^0 polarization.

Note that the three spin components of the Λ^0 polarization can be analyzed independently, by forming $\cos\theta$ distributions with respect to each of the three axes, $\hat{l}$, $\hat{t}$, and $\hat{n}$. Determination of the helicity-dependent polarization components P_l and P_t is made particularly easy, as for each kinematic setting one can form the helicity sum, for which the polarization and the asymmetry must vanish. Thus the sum determines the acceptance with respect to these axes, and allows checks of Monte Carlo simulations and of acceptance matching. For each individual setting one may also determine the helicity-

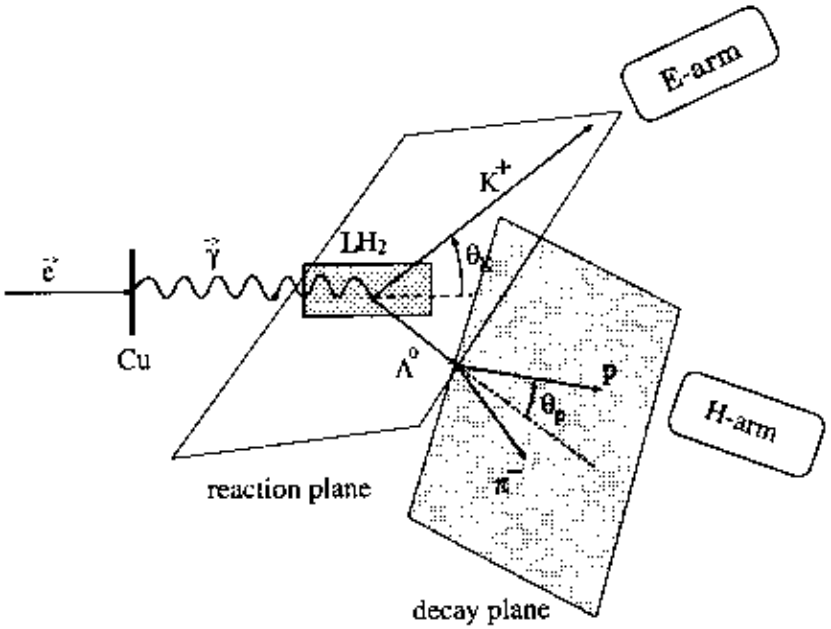

Figure 6: *Basic setup for the $\gamma p \to K^+\Lambda^0$ experiment.*

difference asymmetry, given by $2AP_{At,t}\cos\theta$. In the ratio of the difference to the sum spectrum, the acceptance cancels, and the slope determines the polarization directly from the data, with no leading order corrections. The analysis with respect to the induced polarization component P_{An} will require Monte Carlo acceptance corrections.

2.3 Setup

The basic experimental technique is shown in Fig. 6. The 25 μA, 80% longitudinally polarized electron beam strikes a copper radiator, producing a $\sim 0^{\circ}$ circularly polarized bremsstrahlung photon beam, with maximum energy essentially equal to the electron kinetic energy. The helicity of the high energy photons can be calculated exactly, and is essentially equal to that of the incident electrons. The target, located downstream of the radiator, is irradiated by both the photons and unscattered electrons. Radiator in / out measurements are used to determine the electroproduction background.

The only non-standard piece of equipment in this experiment is the radiator used to generate the bremsstrahlung beam. The radiator construction

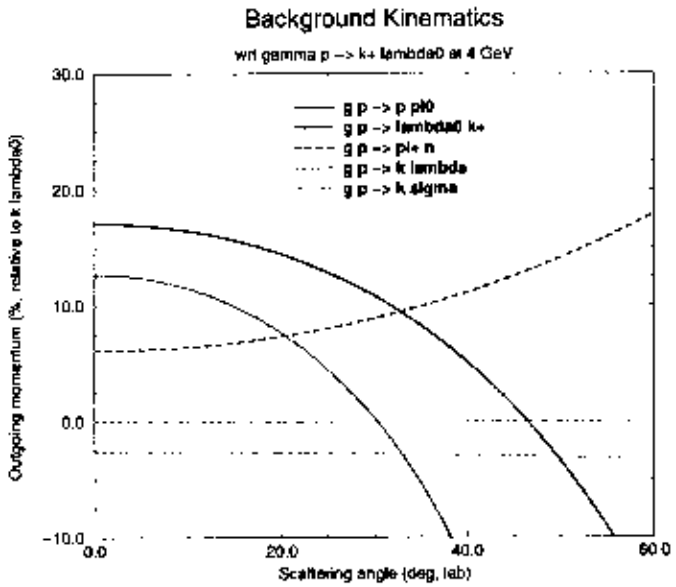

Figure 7: *Relative momentum of positively charged particles from other reactions, as the relative difference from the $\gamma p \rightarrow K^+\Lambda^0$ kaon momenta for the same laboratory angles at an incident energy of 4 GeV. The calculations are for the five reactions in the legend.*

has just been completed by Rutgers University. The radiator has Cu foils up to 6% of a radiation length thick, corresponding to ~1 mm thickness. The radiator will be mounted immediately upstream of the scattering chamber, about 90 cm from the target center. The radiator is not directly seen by the spectrometer.

The two Hall A spectrometers are used to detect K^+ mesons in coincidence with protons from the Λ^0 decay. We will determine all cross sections and polarizations from the K^+p coincidence data. Both Hall A spectrometers have been commissioned and used successfully in several experiments. Some additional optics work may be needed for the current experiment, if we run at momentum settings in which the spectrometers have not previously been operated.

2.4 Singles Rates and Backgrounds

The spectrometers are operated near the endpoint of the bremsstrahlung spectrum. This can be seen in Fig. 7. Since both spectrometers measure positively charged particles, and both are typically at about 85 % of the maximum possible positive charged particle outgoing momentum, background singles rates and random coincidence rates are low. Some experimental indications of this already exist. In Hall A E93-027 measurements of ep elastic scattering, with kinematics similar to those of our 4 GeV, 90 degree center of mass point, hadron arm singles rates were about 400 Hz at 25 μA current. Singles measurements from Hall C HMS [17], with kinematics overlapping our 4 GeV, 70 degree center of mass point, also indicate a singles rate for our kaon spectrometer of about 400 Hz at 25 μA. Neither of these measurements included a photon radiator.

Because the singles rates are low, random coincidences are not a problem, and all true and random coincidences can be read by the data acquisition system. Particle identification information is not needed in the hardware trigger, but may instead be applied to the coincidence data in replay.

2.4.1 Random Coincidences

We assume the radiator approximately doubles the singles rates, leading to singles rates of about 1 kHz at 4 GeV. At this rate, there will be 0.1 Hz of random coincidence triggers in the 100 ns hardware trigger coincidence window; the true coincidence rate at 4 GeV is about the same. In replay, the 2 - 3 ns wide corrected time of flight true coincidence window reduces the random background to less than 3 %. Kinematic reconstructions allow further reduction of the random background, and the out of time data allows a check of the method. For random coincidences, a simple estimate is that the rejection factor for this technique is given by the ratio of spectrometer momentum byte to momentum resolution, a factor of order 1000.

2.4.2 Particle identification

Analysis of the coincidence data will use existing particle identification detectors and information from the spectrometers.

- Measurement of proton time of flight between scintillators within the detector stack determines the velocity β to about 5% on the electron

arm, and 2.5% on the hadron arm, with scintillator S3. This provides proton / meson separation.

- The Aerogel Cerenkovs, with $\beta_{th} \sim 0.976$, have a momentum threshold of 0.63 GeV/c for π, 2.211 GeV/c for K, and 4.21 GeV/c for p. Separation of K^+ from π^+ is good for most of our measurements. Separation of p from π^+ for good for all of our measurements.

- The corrected coincidence time of flight resolution is $\sim$1 ns (FWHM). This is sufficient to easily reject all true coincidences other than proton plus K^+ or π^+ meson. The time of flight difference for K^+ and π^+ ranges from 9 ns at 1 GeV/c to 0.6 ns at 4 GeV/c. The peaks are 3σ apart up to 2.7 GeV/c momentum.

Planned future improvements in scintillator timing and additional Cerenkov detectors will make these measurements easier.

2.4.3 True Coincidence Backgrounds

There are several other reactions that can lead to two positive charged particles, all of which have about the same cross section as $\gamma p \rightarrow K^+\Lambda^0$. These reactions include:

(a) $\gamma p \rightarrow \phi^0 p$; $\phi^0 \rightarrow K^- K^-$

(b) $\gamma p \rightarrow K^+\Sigma^0$; $\Sigma^0 \rightarrow \gamma\Lambda^0$, $\Lambda^0 \rightarrow p\pi^-$,

(c) $\gamma p \rightarrow \pi^-\Delta^{++}$; $\Delta^{++} \rightarrow \pi^+ p$,

(d) $\gamma p \rightarrow \rho^0 p$; $\rho^0 \rightarrow \pi^+\pi^-$

(e) $\gamma p \rightarrow \pi^+\Delta^0$; $\Delta^0 \rightarrow \pi^- p$

Reaction (a) is generally not in our coincidence spectrometer acceptance, because the K^- / π^- mass difference reduces the energy and momentum available to the p and K^+. For reaction (b), one can see from Fig. 7 that the outgoing K^+ has lower energy than it would in the $K^+\Lambda^0$ channel. Reaction (c) is generally out of our acceptance, since the p and π^+ from the Δ^{++} decay go in generally the same direction, rather than into the two spectrometers. Reactions (c), (d), and (e) also have the wrong true coincidence time between the two spectrometers. Finally, all these reactions can be rejected by checking

the kinematic reconstructions of the π^- missing mass (140 MeV) and of the proton momentum in the Λ^0 rest frame (101 MeV/c).

Other reactions are possible, but generally these involve additional particles in the final state, leaving less kinetic energy; thus the reactions are not in our acceptance.

2.5 Monte Carlo

A main feature of this experiment is the coincidence measurement of the K^+ and proton from the Λ decay. Since $\gamma p \to K^+\Lambda^0$ has two-body kinematics, the measured K^+ momentum and direction can be used to reconstruct the photon energy (assuming the direction is along the beamline), and thus the Λ^0 momentum vector. Using the reconstructed Λ^0 plus the measured proton momentum and direction, the decay vertex kinematics are reconstructed along with the π^- missing mass.

The Λ typically travels $\approx$20 cm before decaying, thus the proton trajectory no longer points to the $\gamma p \to K^+\Lambda$ vertex. If not corrected for, the vertical target offset leads to a contribution to the spectrometer resolution. The measurement of scattering angles θ and ϕ, and of the position y_{tg} - the proton trajectory horizontal position projected back to the target - are unchanged.

The proton trajectory can be offset at the target by about 20(cm) $\times$ 0.03(r) = 0.6cm(σ). The momentum resolution is made worse by about:

$$0.6(\mathrm{cm}) \times 1.8 \cdot 10^{-3}(/\mathrm{cm}) \sim 1.1 \times 10^{-3}(\sigma)$$

The factor of $1.8 \cdot 10^{-3}$ includes the magnification and dispersion of the spectrometer. While this resolution is worse than the resolution typically obtained so far, 3×10^{-4} (FWHM), it is sufficient for the purposes of this experiment. We also note that the range in y_{tg} will be increased by about 1 cm, so resolution will be slightly worse, and the ability to use vertex cuts on the coincidence data is lost.

We have performed Monte Carlo simulations of the $\gamma p \to K^+\Lambda^0$, $\Lambda^0 \to p\pi^-$ coincidence measurement. These simulations allow us to study our coverage of the Λ decay cone, and our resolution in reconstruction of the Λ decay. The simulation uses the experimentally determined spectrometer acceptances of about $\pm$28 mr in horizontal angle, $\pm$55 mr in vertical angle, and $\pm$4 % in momentum. Resolutions (rms) are 1 mr in horizontal angle, 2 mr in

vertical angle, and 10^{-4} in momentum. We also offset the momentum of the detected proton, according to the prescription given above, for the individual trajectory of each event. The simulation also includes target and radiator energy loss and multiple scattering effects.

When the Λ^0 decays, the proton is within 3° of the Λ direction, for the higher beam energies and forward Λ angles of this proposal. The size of the decay cone increases to 10° at lower energies and backward Λ angles. Thus, several kinematic settings of the proton spectrometer are needed to sample the decay cone, to determine the Λ^0 polarization. This is confirmed by the Monte Carlo simulation, as shown in Fig. 8. The simple decay cone one expects for the decay is not clear in these figures because the calculations include the momentum and solid angle acceptances of the kaon spectrometer, and a cut on the vertical angle acceptance of the hadron spectrometer, which cannot be adjusted.

Some kinematic reconstructions are shown in Fig. 9. The good missing mass resolution for the π^- allows good background rejection, and the good reconstructed $p\Lambda^0$ decay angle allows precise determination of the Λ^0 rest frame decay angular distribution. We also find (not shown) that the photon energy can be reconstructed to 10 MeV (rms) even at 6 GeV. The $\cos\theta$ distributions demonstrate the independence of the three polarization components.

Further studies are underway to examine in detail the rejection factors available with kinematic reconstructions of random coincidences and of real coincidence reactions with two high energy positively charged particles.

3 Time Estimates

For the kinematics of this proposal, K^+ cross sections are known to about a factor of two. The time estimate in Table 1 assumes a 15 cm (1.08 g/cm^2) liquid hydrogen target. For a point target, the solid angle is slightly greater than 6 msr, and one does not have to consider cuts from the spectrometer y-target acceptance of 10 cm. We approximately account for the reduced acceptance of the extended target by using a 6 msr solid angle with a 7 cm y-target acceptance; thus the rate is reduced at scattering angles greater than about 30°, for which the projection of the target is longer than 7 cm. We assume an 80% longitudinally polarized, 25 μA electron beam, with a 6% radiator for photon flux calculation. We also put in a particle detection /

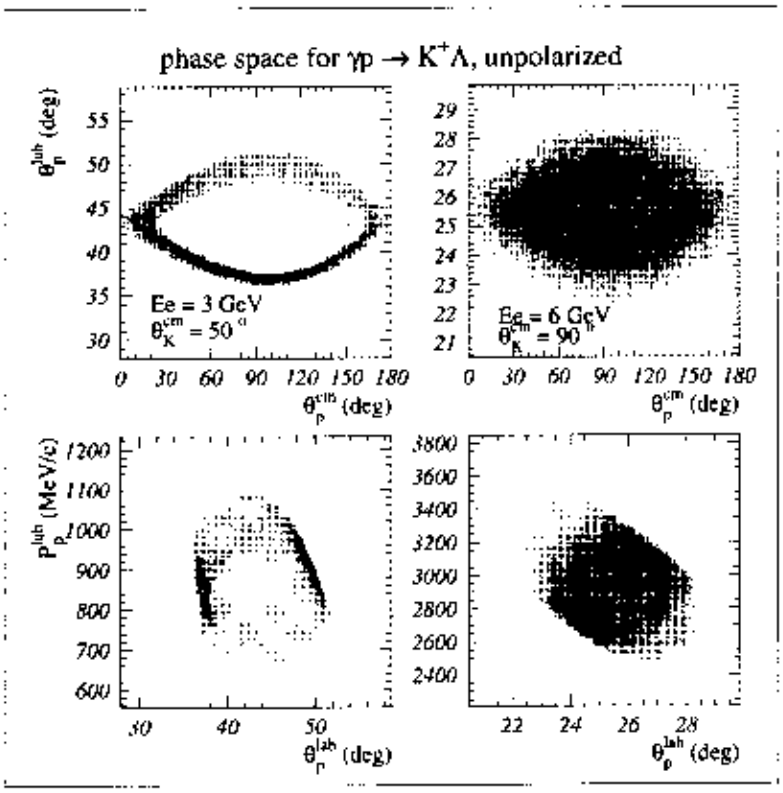

Figure 8: *Monte Carlo simulations of expected proton energies and angles for $\gamma p \rightarrow K^+\Lambda^0$ followed by $\Lambda^0 \rightarrow p\pi^-$ decay. The limits of the distributions are determined by the kaon spectrometer acceptance and the vertical acceptance of the proton spectrometer. The left side panels are for 3 GeV photon energy and 50° center of mass scattering angle. The right side panels are for 6 GeV photon energy and 90° center of mass scattering angle.*

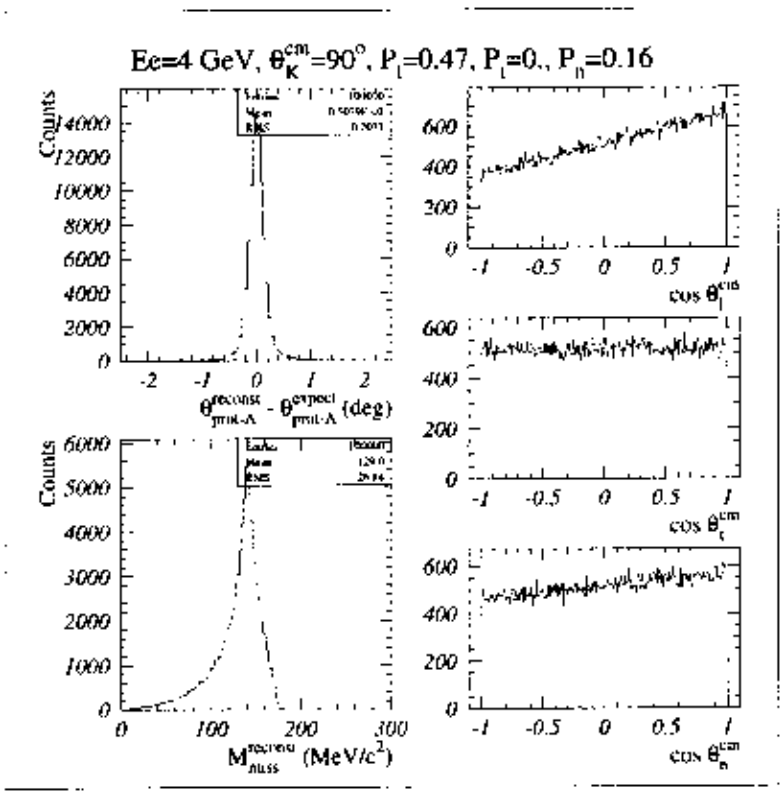

Figure 9: *Monte Carlo simulations for resolutions and polarizations in* $\gamma p \rightarrow K^+\Lambda^0$ *at 4 GeV beam energy and 90° center of mass kaon scattering angle. Top left panel: The reconstruction quality expected for the* Λ^0 *- p laboratory decay angle, in degrees. Bottom left panel: The reconstructed* π *missing mass. Resolution is about 20 MeV. No correction has been made for the offset of the proton trajectory at the target. Right side: Polarization spectra projected to the three spin axes, l, t, and n, in the* Λ^0 *rest frame. The analyzing power is 0.64, and the assumed polarizations are* $P_l = 0.47$, $P_n = 0.16$, *and* $P_t = 0.0$.

tracking efficiency of 80%, and a K^+ survival fraction for each kinematics.

Table 1 shows the kinematics for the $\gamma p \rightarrow K^+\Lambda^0$ reaction. The data taking time request is summarized in Table 2. The time shown is sufficient for detection of a minimum of 400 K^+ *coincidence* events. Because of the width of the Λ decay cone, typically 4 to 10 angle / momentum settings of the proton spectrometer are needed for coincidence measurements, to sample the decay cone sufficiently so that reliable polarizations can be extracted. There are usually 1 - 2 angle settings and 3 - 5 momentum settings for the proton, for each kaon setting. The detection of 400 Λ^0 decay events will be sufficient to determine coincidence cross sections to 5 % statistical uncertainties, which, neglecting systematics, leads to an uncertainty of ≈ 0.1 on the exponent of the scaling power law. It also allows determination of the polarization to $\approx \pm 0.1$.

We assume a minimum data taking time per point of 20 minutes. The time request of Table 2 includes time for radiator out and empty target measurements. The time corresponds to 24 days at 100% beam availability. The overhead time associated with configuration changes is about 3 days, assuming an average of one-half hour for each setting. This leads to a total of $24 + 3 = 27$ days.

We have not asked for time in this proposal for commissioning work. As indicated above, if the spectrometers are being operated in new momentum settings, some optics commissioning work may be needed. Elastic ep scattering data may be needed to setup the coincidence measurement and check our ability to perform absolute cross sections and particle identification. We also plan to extract cross sections for the π^+ meson production background, and the K^+p from Σ^0 decay, when possible.

Table 1 Kinematics and counting time for 500 kaons (not K^+p coincidences) from the $\gamma p \to K^+\Lambda^0$ reaction. The rates are based on existing experimental data, along with additional assumptions specified in the text. Measurements are not possible at 6 GeV, 50° and 130°, due to the maximum momentum measurable in the spectrometers.

E_γ [GeV]	θ_{cm} [deg]	θ_{K^+} [deg-lab]	p_{K^+} [GeV/c]	time [hours]	θ_p range [deg]	p_p range [GeV/c]
3	50.	18.47	2.281	0.01	43.32±10.29	0.899±0.224
	70.	27.14	1.943	0.03	36.44±7.30	1.274±0.273
	90.	37.37	1.554	0.11	29.10±5.63	1.656±0.327
	110.	50.11	1.155	0.38	22.04±4.63	2.016±0.382
	130.	67.02	0.785	1.87	15.40±4.02	2.323±0.430
4	50.	16.57	3.122	0.03	43.50±8.41	1.104±0.250
	70.	24.46	2.637	0.10	35.51±5.81	1.605±0.320
	90.	33.94	2.081	0.30	27.81±4.39	2.126±0.399
	110.	46.03	1.517	0.91	20.78±3.56	2.627±0.479
	130.	62.60	1.003	3.86	14.39±3.06	3.057±0.549
5	50.	15.12	3.954	0.07	42.84±7.18	1.295±0.276
	70.	22.40	3.321	0.27	34.24±4.86	1.920±0.367
	90.	31.22	2.598	0.77	26.44±3.62	2.582±0.472
	110.	42.68	1.867	2.06	19.58±2.90	3.223±0.576
	130.	58.76	1.206	8.03	13.48±2.47	3.779±0.668
6	70.	20.76	4.001	0.63	32.95±4.19	2.227±0.415
	90.	29.05	3.109	1.76	25.17±3.08	3.030±0.544
	110.	39.93	2.210	4.46	18.52±2.45	3.813±0.674

Table 2 Summary of beam time request. The times given are aimed for the number of coincidence (K^+, p) in the table. This includes the factor of 63.9% Λ^0 decay into the π^- p channel. We assume a minimum data taking for each point of 20 minutes. We double the data time to allow for radiator out and empty target subtractions.

E_e [GeV]	θ_{cm} [deg]	coinc (K^+,P)	time [hours]	total time [hours]	
3.0	50.	11000	3.3	6.6	
	70.	2700	3.3	6.6	
	90.	1000	3.8	7.6	
	110.	1000	9.3	18.6	
	130.	1000	39.6	79.2	
	all θ		59.3		118.6
4.0	50.	3500	3.3	6.6	
	70.	1000	3.5	7.0	
	90.	1000	5.2	10.4	
	110.	1000	15.8	31.6	
	130.	400	27.1	54.2	
	all θ		55.0		110.
5.0	50.	1300	3.3	6.6	
	70.	1000	6.6	13.2	
	90.	1000	13.4	26.8	
	110.	1000	36.4	72.8	
	130.	400	44.5	89.0	
	all θ		104.2		208.4
6.0	70.	1000	13.2	26.4	
	90.	1000	25.0	50.0	
	110.	400	25.0	50.0	
	all θ		63.2		126.4
all E_γ	all θ		282		564 = 24 days
total configuration change(0.5 hrs/setting)					70.5 = 3 days

4 Summary

We propose a coincidence measurement of K^+ and p from the $\vec{\gamma}p \to K^+\vec{\Lambda}^0$, $\Lambda^0 \to p\pi^-$ reaction, for photon energies from 3 to 6 GeV, and for K^+ angles in the center of mass from 50° to 130°. The polarization measurements will be the first polarization data in this energy and angle regime, and the cross section measurements are significant improvements over previous data. The uncertainties in the data will allow a selection of quark-based models for the reaction.

Measureable deviations from the constituent counting rules are predicted in the framework of diquark models and non-forward parton distributions. We may finally be able to resolve the long standing puzzle of why data appear to follow pQCD scaling, in a regime where pQCD is not generally expected to be applicable.

Helicity conservation will be tested by measurement of the induced polarization P and polarization transfer C_x, which result from the imaginary and real parts of the helicity-violating interference. Since the spin of the Λ is carried by the s quark, the models predict a large polarization transfer C_z. The combination of cross section and polarization measurements provides strong constraints on the underlying reaction mechanisms.

References

[1] A. M. Boyarski *et al.*, Phys. Rev. Lett. **22**, 1131 (1969).

[2] G. Vogel *et al.*, Phys. Lett. B **40**, 513 (1972).

[3] R. L. Anderson *et al.*, Phys. Rev. D **14**, 679 (1976).

[4] S. J. Brodsky and G. R. Farrar, Phys. Rev. Lett. **31**, 1153 (1973); V. A. Mateev *et al.*, Lett. Nuovo Cimento **7**, 719 (1973); S. J. Brodsky and G. R. Farrar, Phys. Rev. D **11**, 1309 (1975). Also see S. J. Brodsky and G. P. Lepage in *Perturbative Quantum Chromodynamics*, edited by A. Mueller, page 93 (World Scientific, Singapore, 1989).

[5] N. Isgur and C. Llewellyn Smith, Nucl. Phys. **B317**, 526 (1989); A. V. Radyushkin, Nucl. Phys. **A523**, 141c (1991).

[6] M. Guidal, J.-M. Laget, and M. Vanderhaeghen, Phys. Lett. B **400**, 6 (1997).

[7] I. S. Barker, A. Donnachie, and J. K. Storrow, Nucl. Phys. **B95**, 347 (1975).

[8] C. E. Carlson and M. Chachkhunashvili, Phys. Rev. D **45**, 2555 (1992).

[9] A. Afanasev, Carl E. Carlson, and Christian Wahlquist, Phys. Lett. B **398**, 393 (1997); *ibid.* hep-ph/9701215.

[10] G.R. Farrar, K. Huleihel, and H. Zhang, Nucl. Phys. B **349**, 655 (1991).

[11] P. Kroll, M. Schurmann, K. Passek, and W. Schweiger, Phys. Rev. D **55**, 4315 (1997); *ibid.* hep-ph/9604353.

[12] X. Ji, Phys. Rev. D **55**, 7114 (1997); A. Radyushkin, Phys. Rev. D **56**, 5524 (1997).

[13] A. Radyushkin, preprint JLAB-THY-98-10, hep-ph/9803316, private communication.

[14] L. Mankiewicz *et al.*, hep-ph/9711227; J. Collins, L. Frankfurt, and M. Strikman, Phys. Rev. D **56**, 2982-3006 (1997) and hep-ph/9611433.

[15] A. Afanasev, private communication.

[16] M. Vanderhaeghen, DAPNIA/SPhN-97-42.

[17] Jefferson Lab proposal E94-014, spokespersons P. Stoler and J. Napolitano. We thank V. Frolov for providing the information.